

基于光强迭代的单幅干涉图相位提取方法

张翔宇, 田爱玲, 刘志强, 王红军, 刘丙才, 朱学亮*

西安工业大学光电工程学院, 陕西省薄膜技术与光学检测重点实验室, 陕西 西安 710021

摘要 提出了一种基于光强迭代的单幅干涉图相位提取方法, 实现了对单幅干涉条纹图的高精度相位提取。首先通过对原始干涉图进行预处理得到初始相位; 将初始相位引入到干涉条纹图的强度表达式中, 利用最小二乘法初步得到背景光和调制光; 再将初步估计的背景光和调制光代入最初干涉图的强度表达式中以求解待测相位, 比较得到的待测相位和初始相位, 若不满足迭代精度要求, 则重复上述相位求解过程并实现迭代, 若求解的相位与初始相位的均方根差值满足收敛条件, 则停止迭代。进行仿真和实验研究, 得到的 $\Phi 100$ mm口径平面元件的测量提取结果与实际相位一致。结果表明, 该方法在具有较高检测精度的同时能够有效地保证算法的稳定性。

关键词 测量; 干涉测量; 单幅干涉图; 迭代方法; 最小二乘法

中图分类号 O436 **文献标志码** A

DOI: 10.3788/AOS231891

1 引言

精密光学元件广泛应用于各种光学装置中, 光学元件的面形质量直接影响了光学装置的性能, 因此光学元件面形检测具有重要意义^[1-2]。干涉测量法是公认的最有效的面形检测方法^[3], 其中相移干涉法具有更高的检测精度, 在连续采集多幅具有相位差的干涉图时, 受限于实现移相部件的性能, 同时容易受到环境中存在的机械振动、空气扰动等客观因素的干扰^[4], 其检测精度不高, 故不适用于生产现场检测。

研究人员提出了将载波干涉法与傅里叶分析技术相结合的方法^[5-6], 该方法仅需一幅干涉图即可获得被测相位信息, 对噪声的抑制效果较好, 比较适合对时间响应要求较高的场合。但傅里叶变换法处理干涉图时对干涉图的载频数和窗函数有严格要求^[7-8], 如果被测面高低变化较大, 条纹就会出现堆积现象, 造成采样不足^[9]; Tian等^[10]提出了基于Zernike多项式拟合的方法以对单幅干涉图进行相位求解, 相较于传统相移方法, 该方法的局限更少但精度较低; Takeda等^[11]提出了基于傅里叶分析进行相位提取的方法, 该方法具有自动去噪、稳定性高的优点, 但是傅里叶变换法需要添加较大的载波, 从而导致倾斜方向的边缘误差较大; Qian^[12]提出了二维窗口傅里叶变换法进行条纹图分析, 该方法具有较好的降噪能力和相位恢复能力, 但是频谱被阈值化时会轻微破坏有用信息, 造成相位提取精度下

降^[13-15]; Servin等^[16]提出的二维正则化相位跟随技术是一种很有效的方法, 该方法具有结果无跳变、自动去除高频噪声的优点, 但在求解相位前需要对干涉图进行预处理, 这会带来处理时间长、恢复精度低的缺点; 刘东等^[17]通过对二维正则化相位跟随技术求解的结果进行最优解的二次搜索, 进一步提高了该方法的求解精度, 但由于进行了二次求解, 算法较为复杂。

为解决上述对单幅干涉图相位提取的问题, 本文提出一种新的基于光强迭代的单幅干涉图相位提取方法, 开展仿真和实验研究, 并分析算法的稳定性。

2 基本原理

根据光干涉原理, 两个相干波面发生干涉时, 其干涉图像的光强分布为

$$I(x, y) = a(x, y) + b(x, y) \cos[\phi(x, y)], \quad (1)$$

式中: $a(x, y)$ 为干涉图的背景光强; $b(x, y)$ 为干涉条纹的幅值调制; $\phi(x, y)$ 为物体变形的相位分布函数。式(1)中 $a(x, y)$ 、 $b(x, y)$ 均为未知量, $I(x, y)$ 为已知的干涉图的强度信息。为了提取出 $\phi(x, y)$, 需要减少未知量, 因此需要对原始干涉图进行二值化处理^[18]。采用区域Berssen算法, 以 (x, y) 为中心, 窗口大小为 $(2w + 1) \text{ pixel} \times (2w + 1) \text{ pixel}$, 其中, w 为常数, 通过修改 w 可以控制窗口大小, 该区域内的阈值为

收稿日期: 2023-12-05; 修回日期: 2024-01-02; 录用日期: 2024-01-10; 网络首发日期: 2024-02-20

基金项目: 陕西省科技厅项目(2023KXJ-066)

通信作者: *zhuxueliang@xatu.edu.cn

$$T(x, y) = \frac{1}{2} \left[\max_{-w \leq k, i \leq w} I(x+k, y+i) + \min_{-w \leq k, i \leq w} I(x+k, y+i) \right], \quad (2)$$

$$I'(x, y) = \begin{cases} 0, & I(x, y) < T(x, y) \\ 1, & I(x, y) \geq T(x, y) \end{cases}, \quad (3)$$

$$\phi'(x, y) = \begin{cases} 0, & I'(x, y) = 0 \\ \pi, & I'(x, y) = 1 \end{cases} \quad (4)$$

此时 $\phi'(x, y)$ 即为近似的包裹相位。通过对 $\phi'(x, y)$ 进行解包裹处理, 得到阶梯形的初始相位 $\phi^{(0)}(x, y)$, 实际情况下背景光和调制光为高斯形式, 分别为

$$a(x, y) = c_1 \exp[(x-h)^2 + (y-h)^2], \quad (5)$$

$$b(x, y) = c_2 \exp[(x-h)^2 + (y-h)^2], \quad (6)$$

式中: c_1, c_2 为常数; h 为常数, 表示高斯光源的中心位置。将式(5)、(6)代入干涉条纹图的强度表达式

[式(1)]中, 得到

$$I(x, y) = c_1 \exp[(x-h)^2 + (y-h)^2] + c_2 \exp[(x-h)^2 + (y-h)^2] \cos \phi(x, y), \quad (7)$$

式中: $I(x, y)$ 为采集到的干涉图。为方便计算, 令 $h=0$, 即高斯光源在干涉图中心位置, 式(7)可变换为

$$I(x, y) = c_1 \exp(x^2 + y^2) + c_2 \exp(x^2 + y^2) \cos \phi(x, y). \quad (8)$$

基于光强迭代法对待测相位进行迭代求解, 具体流程如下:

$$A(c_1, c_2) = \sum_{x=1, y=1}^n [c_1 \exp(x^2 + y^2) + c_2 \exp(x^2 + y^2) \times \cos \phi^{(i-1)}(x, y) - I(x, y)]^2, \quad (9)$$

式中: i 为迭代次数。第一次通过原始相位进行背景光和调制光计算时, 将阶梯形初始相位 $\phi^{(0)}(x, y)$ 代入 $\phi^{(i-1)}(x, y)$ 的位置:

$$\frac{\partial A}{\partial c_1} = \sum_{x=1, y=1}^n [c_1 \exp(x^2 + y^2) + c_2 \exp(x^2 + y^2) \cos \phi^{(i-1)}(x, y) - I(x, y)] = 0, \quad (10)$$

$$\frac{\partial A}{\partial c_2} = \sum_{x=1, y=1}^n [c_1 \exp(x^2 + y^2) + c_2 \exp(x^2 + y^2) \cos \phi^{(i-1)}(x, y) - I(x, y)] = 0. \quad (11)$$

条纹图大小为 $n \text{ pixel} \times n \text{ pixel}$, 即

$$\mathbf{B} = \begin{bmatrix} \sum_{x=1, y=1}^n \exp(x^2 + y^2) & \sum_{x=1, y=1}^n \exp(x^2 + y^2) \cos \phi^{(i-1)}(x, y) \\ \sum_{x=1, y=1}^n \exp(x^2 + y^2) \cos \phi^{(i-1)}(x, y) & \sum_{x=1, y=1}^n \exp(x^2 + y^2) \cos^2 \phi^{(i-1)}(x, y) \end{bmatrix}, \quad (12)$$

$$\mathbf{C} = [c_1^{(i)} \ c_2^{(i)}], \quad (13)$$

$$\mathbf{Y} = \begin{bmatrix} \sum_{x=1, y=1}^n I(x, y) \\ \sum_{x=1, y=1}^n \cos \phi^{(i-1)}(x, y) I(x, y) \end{bmatrix}, \quad (14)$$

则得: $\mathbf{BC}^T = \mathbf{Y}$, 从而有

$$\mathbf{C}^T = \mathbf{B}^{-1} \mathbf{Y}, \quad (15)$$

$$a^{(i)}(x, y) = c_1^{(i)} \exp(x^2 + y^2), \quad (16)$$

$$b^{(i)}(x, y) = c_2^{(i)} \exp(x^2 + y^2), \quad (17)$$

$$\phi^{(i)}(x, y) = \arccos \frac{I(x, y) - a^{(i)}(x, y)}{b^{(i)}(x, y)}, \quad (18)$$

式中: $a^{(i)}(x, y), b^{(i)}(x, y)$ 分别为第 i 次运算得到的背景光和调制光; $\phi^{(i)}(x, y)$ 为第 i 次运算得到的待测相位。迭代时将更新后的 $\phi^{(i)}(x, y)$ 代入式(12):

$$\delta = \sqrt{\frac{1}{n} \sum [\phi^{(i)}(x, y) - \phi^{(i-1)}(x, y)]^2} \leq \epsilon, \quad (19)$$

式中: δ 为均方根差; ϵ 为手动设定的收敛阈值。

式(12)~(19)为迭代公式, 式(19)为收敛条件的判别: 若 $\delta \leq \epsilon$, 则停止迭代; 若不满足迭代条件, 则将求解出的 $\phi^{(i)}(x, y)$ 再次代入式(12)的 $\phi^{(i-1)}(x, y)$ 中, 重复式(12)~(19)。当 δ 不再下降时, 迭代停止, 此时 $\phi^{(i)}(x, y)$ 即为最终提取的相位。对 $\phi^{(i)}(x, y)$ 进行解包裹^[19-20]和 Zernike 多项式拟合^[21-23], 得到最终面形。在多项式求解中, 基于光强迭代的单幅干涉图重建方法能够实现待测相位的高精度提取。

该方法可推广到不同形式的背景光和调制光, 从而更加精准地对待测相位进行求解。整体流程为对原始干涉图进行二值化处理得到包裹相位, 进行相位解包裹得到初始相位, 再通过干涉强度表达式、利用最小二乘法得到背景光和调制光的估计值, 利用估计值计算待测相位, 将待测相位和初始相位进行比较, 比较结果可作为迭代依据, 最终得到满足收敛条件的待测相位。算法流程如图 1 所示。

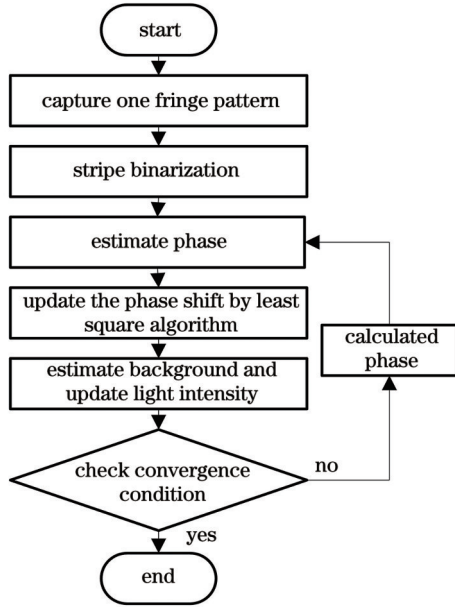


图1 算法流程图

Fig. 1 Algorithm flow chart

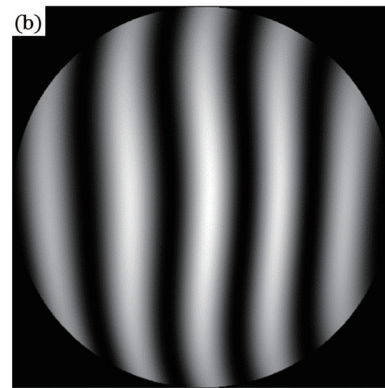
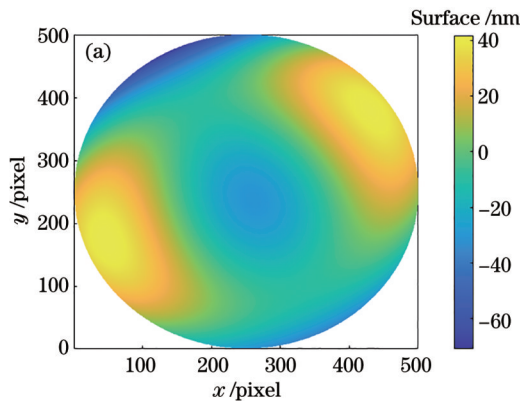


图2 原始面形和仿真的条纹图。(a)原始面形;(b)仿真生成对应的干涉图

Fig. 2 Original surface shape and simulated stripe pattern. (a) Original surface shape; (b) simulated corresponding interferogram

通过近百组仿真模拟,当PV和RMS达到纳米级和亚纳米级时 δ 在 $1 \times 10^{-3} \sim 1 \times 10^{-2}$ 的区间内波动,为保证求解精度且不影响运算效率,避免算法过度迭代,将收敛条件 ϵ 设置为 1×10^{-2} 后进行后续的迭代过程。具体仿真结果如图4所示。该迭代法的测量结果如图4(a)所示,傅里叶变换方法的测量结果如图4(b)所示。

最终 $\delta = 1.2 \times 10^{-2}$ 时,停止迭代。本文提出的迭代法和傅里叶变换法重建的相位与参考相位的残差PV分别为5.55 nm和7.56 nm,RMS分别为0.84 nm和1.09 nm。可知本文所提方法相较于傅里叶变换法检测精度有较大提升。

3.2 随机噪声对算法的影响

该方法是一种对相位进行预测后再进行迭代的方法。为验证该方法对噪声的敏感程度,通过对原始仿真干涉图添加单一白噪声和混合噪声的手段来探究不同信噪比的单一噪声和混合噪声对最终重建精度的影

3 仿真分析

3.1 无噪声条件下的仿真分析

利用36项Zernike多项式模拟一个马鞍形的面形。图2(a)为仿真的原始面形,基于斐索光路干涉原理将图2(a)中面形进行一定倾斜,参考面为理想平面,生成如图2(b)所示的单幅干涉条纹。该仿真面形的峰谷(PV)值为98.72 nm,均方根(RMS)值为20.57 nm, $\lambda = 632.8$ nm。

对图2(b)采用局部区域Berssen算法进行二值化处理,得到图3(a),通过对二值化处理后的近似相位图进行解包裹得到如图3(c)所示的阶梯形初始相位,图3(b)、(d)分别为包裹相位和解包裹相位第250行数据图。将Berssen算法的局部区域设定为5 pixel \times 5 pixel时最终重建面形的PV为8.38 nm,RMS为1.02 nm。将区域设定为3 pixel \times 3 pixel时,重建面形的PV为5.55 nm,RMS为0.84 nm,故算法二值化处理时采用3 pixel \times 3 pixel的局部区域Berssen算法。

响。分别使用两种方法得到重建相位的残差值。图5为不同信噪比的单一噪声对两种方法重建相位的残差值的影响,图6为混合噪声对两种方法重建相位的残差值的影响。

由图5、图6可以看出:由于傅里叶变换法使用了频谱转换,并进行了滤波,故无论是单一白噪声还是混合噪声对于面形重建精度的影响都较小,本文方法对原始干涉图进行去噪处理,利用迭代法对相位进行求解时,不使用频谱滤波也能对单一白噪声或者混合噪声具有很好的滤波效果。由图5、6可知残差的PV值和RMS值变化并不明显,这表明本文方法对噪声不敏感,具有较好的稳定性。

3.3 倾斜程度对算法的影响

在生产现场环境中,设备自身产生的振动、气流扰动和气温变化等客观因素,导致在检测时会获取到不同条纹数量的干涉图。如传统四步相移方法需要尽可

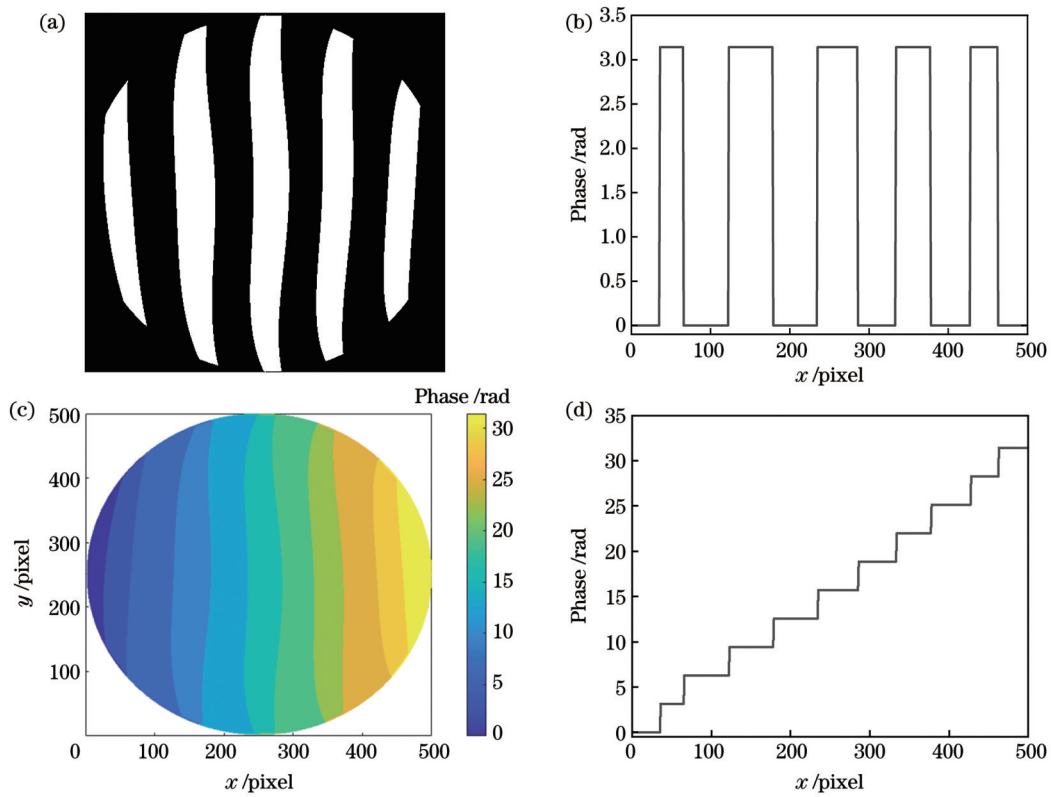


图 3 初始相位。(a)二值化图像;(b)第 250 行包裹相位;(c)解包裹相位;(d)第 250 行解包裹相位
Fig. 3 Original phases. (a) Binary image; (b) wrapped phase of line 250; (c) unwrapping phase; (d) unwrapped phase of line 250

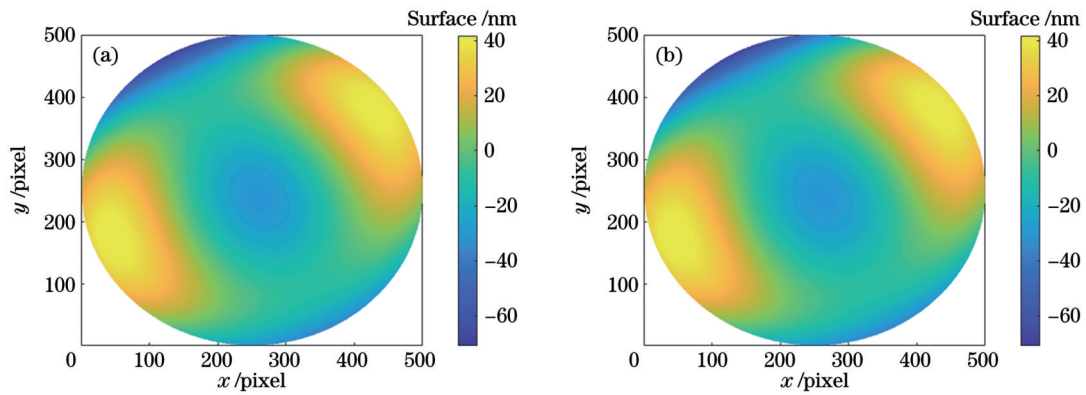


图 4 重建相位图。(a)本文方法重建的相位;(b)傅里叶变换法重建的相位
Fig. 4 Reconstructed phase maps. (a) Reconstructed phase of our method; (b) reconstructed phase of Fourier method

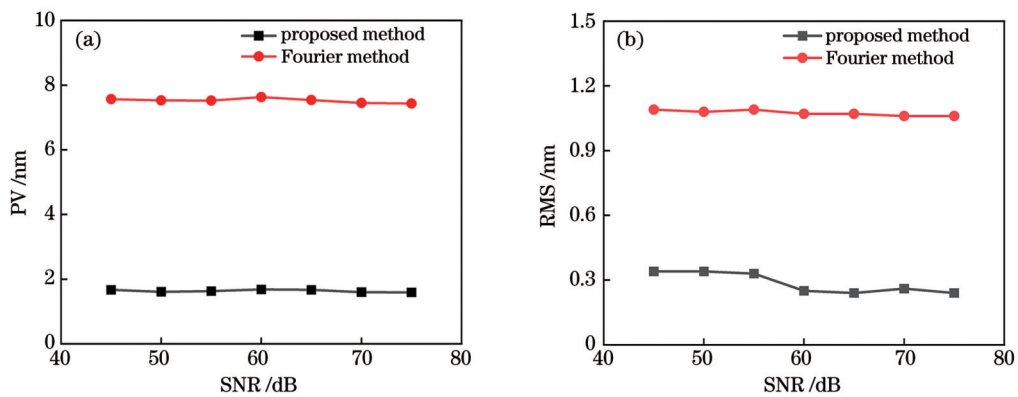


图 5 单一噪声对残差的影响。(a)单一噪声对应的 PV 值;(b)单一噪声对应的 RMS 值
Fig. 5 Figures of impact of single noise on residual. (a) PV corresponding to single noise; (b) RMS corresponding to single noise

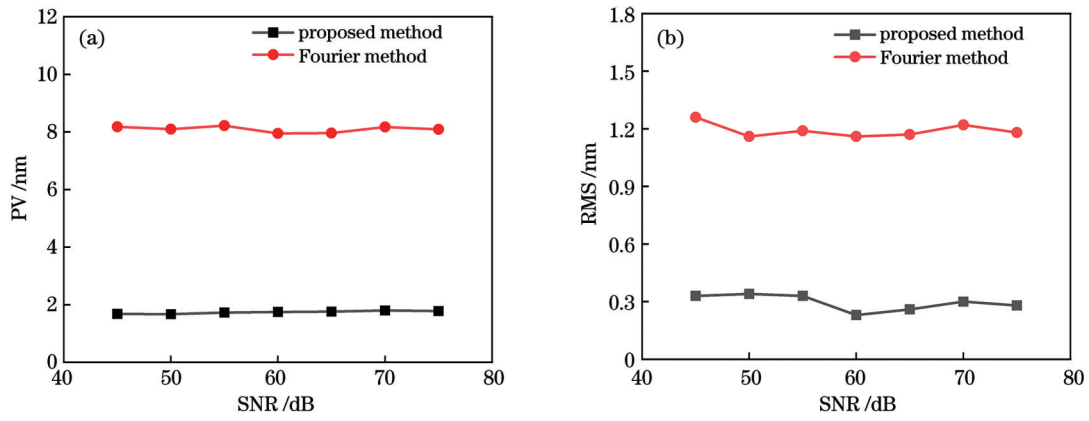


图 6 混合噪声对残差的影响。(a)混合噪声对应的PV值;(b)混合噪声对应的RMS值

Fig. 6 Figures of impact of mixed noise on residual. (a) PV corresponding to mixed noise; (b) RMS corresponding to mixed noise

能少的条纹图以减少载波影响,而傅里叶变换法需要更多的条纹以便进行频域处理。为探究倾斜程度对算法的影响,利用Zernike多项式进行面形仿真,在36项Zernike系数中,第2、3项系数决定面形沿x轴和y轴的倾斜程度,为量化条纹数量,在仿真时采用改变第2项

Zernike系数的方法来仿真平面,即只改变x轴的倾斜程度。为验证不同倾斜系数的影响,仿真了倾斜系数为1~100共100组数据的情况。由于篇幅所限,仅展示9组结果。干涉图如图7所示。图8为针对不同干涉图重建出的面形的残差随系数的变化图。

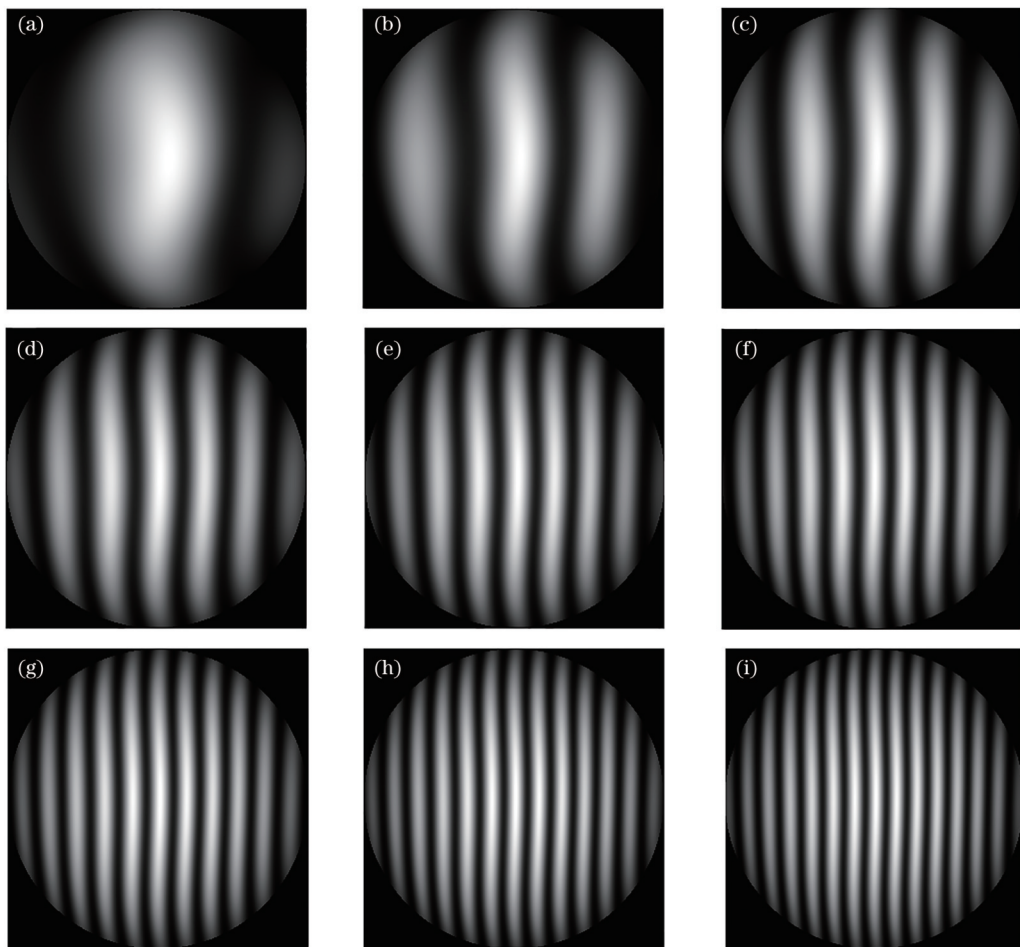


图 7 不同倾斜系数的条纹图。(a)倾斜系数为5;(b)倾斜系数为10;(c)倾斜系数为15;(d)倾斜系数为20;(e)倾斜系数为25;(f)倾斜系数为30;(g)倾斜系数为35;(h)倾斜系数为40;(i)倾斜系数为45

Fig. 7 Fringe patterns with different tilt coefficients. (a) Tilt coefficient is 5; (b) tilt coefficient is 10; (c) tilt coefficient is 15; (d) tilt coefficient is 20; (e) tilt coefficient is 25; (f) tilt coefficient is 30; (g) tilt coefficient is 35; (h) tilt coefficient is 40; (i) tilt coefficient is 45

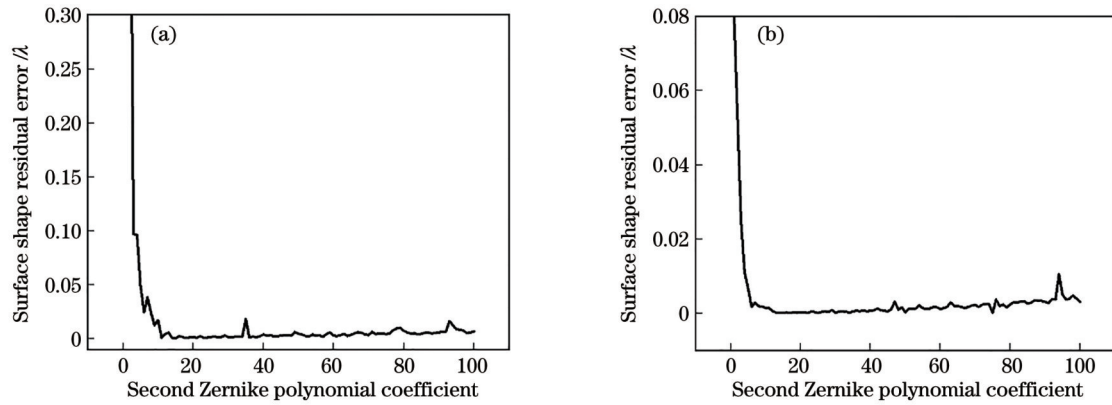


图 8 残差随第 2 项 Zernike 多项式系数的变化图。(a)PV 随第 2 项 Zernike 多项式系数的变化图;(b)RMS 随第 2 项 Zernike 多项式系数的变化图

Fig. 8 Residual varying with the second Zernike polynomial coefficient. (a) PV varying with the second Zernike polynomial coefficient; (b) RMS varying with the second Zernike polynomial coefficient

由上述结果可知,第二项 Zernike 多项式系数在 15 时对应 4~5 条纹,本文提出的基于光强迭代的单幅干涉图相位提取方法所求得的面形残差 PV 值最小为 0.057 nm, RMS 值为 0.013 nm。说明本文的波面重建算法对单幅干涉条纹图有较好的相位提取能力,对 3 条纹以上的单幅干涉图均有较好的相位提取能力,面形倾斜程度对算法的求解精度影响并不大。通过 100 组仿真,该算法对 4~5 条纹的相位提取精度最高。

4 实验结果

为验证迭代方法的实际应用能力,选用 ZYGO-Verifire PE 移相干涉仪进行对比测量。被测对象选用 $\Phi 100$ mm 的平面元件,设置收敛条件为 $\epsilon = 1 \times 10^{-2}$ 。

在温度为 23 °C、空气湿度为 75.3% 的实验环境下,使用标准气浮平台并采用 ZYGO-Verifire PE 移相干涉仪采集到的干涉图如图 9(a)所示,测得该元件的

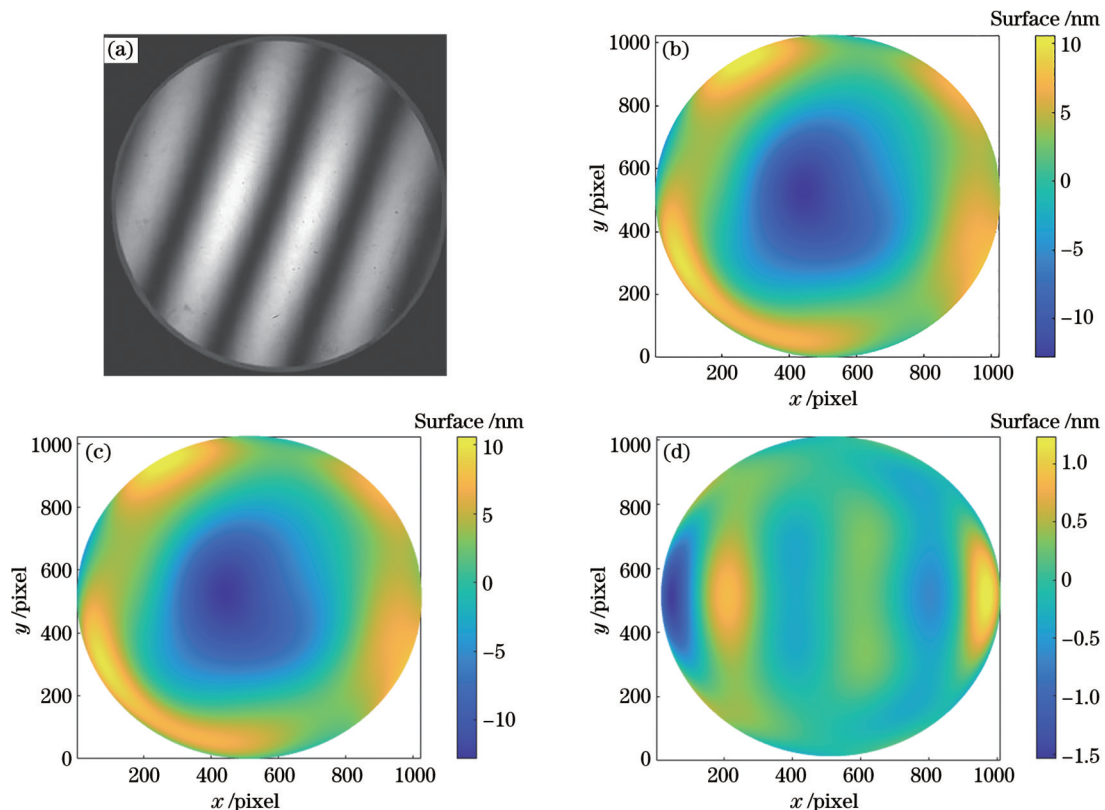


图 9 实验测量得到的相位及残差图。(a)原始干涉图;(b)ZYGO-Verifire PE 移相干涉仪提取的相位;(c)本文方法提取的相位;(d)相位残差

Fig. 9 Phase and residual plots measured in experiment. (a) Original interferogram; (b) phase obtained by ZYGO-Verifire PE phase-shifting interferometer; (c) phase obtained by our method; (d) phase residual

面形分布如图 9(b)所示,针对使用 ZYGO-Verifire PE 相移干涉仪采集到的单幅干涉图,采用光强迭代法求解相位,最终重建的面形如图 9(c)所示,将图 9(b)作为该元件面形分布的参考值,图 9(d)是本文方法求得结果与参考值的差,即相位残差。图 9(a)~(d)的 PV 值和 RMS 值如表 1 所示。上述研究表明本文方法所得相位分布和四步相移方法所得相位分布是一致的, PV 值相差 0.63 nm, RMS 值相差 0.13 nm, 相位残差的 PV 值和 RMS 值分别为 2.49 nm 和 0.35 nm, 均小于参考值的 1/10, 这表明本文方法能从单幅条纹中有效提取相位信息。

表 1 相位及相位误差的 PV 值和 RMS 值
Table 1 PV and RMS values of phase and phase error

Parameter	PV /nm	RMS /nm
Phase by ZYGO-Verifire PE phase-shifting interferometer	22.15	5.38
Phase by our method	22.78	5.51
Phase error	2.49	0.35
Absolute error	0.63	0.13

5 结 论

本文提出了一种基于光强迭代法的相位求解方法,通过对原始干涉图进行二值化处理并进行相位解包裹得到初始相位,再通过干涉强度表达式利用最小二乘法初步估计背景光和调制光,利用干涉强度表达式的变式计算待测相位,将待测相位和初始相位的比较结果作为收敛判断,用不满足精度要求的待测相位取代初始相位,对背景光和调制光进行更新并重复相位求解过程,通过光强迭代实现了从单幅干涉图中提取相位。本研究从求解精度、抗噪能力、算法稳定性等方面进行仿真分析。对 $\Phi 100$ mm 平面元件进行实验测量,实验结果表明本文方法求解的相位分布与四步相移算法所求相位一致,相位残差的 PV 值和 RMS 值分别为 2.49 nm 和 0.35 nm,说明本文方法能从单幅条纹中有效提取相位分布,具有高稳定性和高效率的优势,能够满足车间现场环境的检测需求。

参 考 文 献

- 侯溪, 张师, 胡小川, 等. 超高精度面形干涉检测技术进展[J]. 光电工程, 2020, 47(8): 200209.
Hou X, Zhang S, Hu X C, et al. The research progress of surface interferometric measurement with higher accuracy[J]. Opto-Electronic Engineering, 2020, 47(8): 200209.
- 张梦瑶, 田爱玲, 王大森, 等. 基于逆向优化策略的面形绝对检测平移量研究[J]. 中国激光, 2022, 49(18): 1804003.
Zhang M Y, Tian A L, Wang D S, et al. Translation of surface shape absolute testing based on reverse optimization strategy[J]. Chinese Journal of Lasers, 2022, 49(18): 1804003.
- 王贤敏, 刘东, 臧仲明, 等. 可用于单幅闭合干涉图相位恢复的正则化相位跟随技术[J]. 中国光学, 2019, 12(4): 719-730.

- Wang X M, Liu D, Zang Z M, et al. The regularized phase tracking technique used in single closed interferogram phase retrieval[J]. Chinese Optics, 2019, 12(4): 719-730.
- 陈柔婧, 韩森, 康岩辉, 等. 一种小幅度步距相移干涉算法的相移误差分析[J]. 光子学报, 2022, 51(11): 1112003.
Chen R J, Han S, Kang Y H, et al. Phase shift error analysis of a phase-shifting interference algorithm with small phase step size [J]. Acta Photonica Sinica, 2022, 51(11): 1112003.
- Guo R H, Liao Z S, Li J X, et al. Optical homogeneity measurement of parallel plates by wavelength-tuning interferometry using nonuniform fast Fourier transform[J]. Optics Express, 2019, 27(9): 13072-13082.
- 单小琴, 朱日宏, 李建欣. 基于二维傅里叶变换的单帧干涉图相位提取方法[J]. 应用光学, 2013, 34(5): 802-808.
Shan X Q, Zhu R H, Li J X. Phase extraction for single frame interferogram based on 2D Fourier transform[J]. Journal of Applied Optics, 2013, 34(5): 802-808.
- Qian K M. Applications of windowed Fourier fringe analysis in optical measurement: a review[J]. Optics and Lasers in Engineering, 2015, 66: 67-73.
- Qian K M. On window size selection in the windowed Fourier ridges algorithm[J]. Optics and Lasers in Engineering, 2007, 45(12): 1186-1192.
- 田爱玲, 刘婷, 刘剑, 等. 单幅干涉条纹图的高精度波面重建技术[J]. 红外与激光工程, 2015, 44(4): 1203-1207.
Tian A L, Liu T, Liu J, et al. High precision wavefront reconstruction technology for single interferogram[J]. Infrared and Laser Engineering, 2015, 44(4): 1203-1207.
- Tian C, Yang Y Y, Wei T, et al. Demodulation of a single-image interferogram using a Zernike-polynomial-based phase-fitting technique with a differential evolution algorithm[J]. Optics Letters, 2011, 36(12): 2318-2320.
- Takeda M, Ina H, Kobayashi S. Fourier-transform method of fringe-pattern analysis for computer-based topography and interferometry[J]. Journal of the Optical Society of America, 1982, 72(1): 156-160.
- Qian K M. Two-dimensional windowed Fourier transform for fringe pattern analysis: principles, applications and implementations[J]. Optics and Lasers in Engineering, 2007, 45(2): 304-317.
- Qian K M. Windowed Fourier transform for fringe pattern analysis[J]. Applied Optics, 2004, 43(13): 2695-2702.
- Qian K M. Windowed Fourier transform for fringe pattern analysis: addendum[J]. Applied Optics, 2004, 43(17): 3472-3473.
- Qian K M, Seah H S, Asundi K A. Filtering the complex field in phase shifting interferometry[J]. Optical Engineering, 2003, 42(10): 2792-2793.
- Servin M, Marroquin J L, Cuevas F J. Demodulation of a single interferogram by use of a two-dimensional regularized phase-tracking technique[J]. Applied Optics, 1997, 36(19): 4540-4548.
- 刘东, 杨甬英, 田超, 等. 高精度单幅闭合条纹干涉图相位重构技术[J]. 中国激光, 2010, 37(2): 531-536.
Liu D, Yang Y Y, Tian C, et al. Study on phase retrieval from single close fringe pattern with high precision[J]. Chinese Journal of Lasers, 2010, 37(2): 531-536.
- 贾仁庆, 殷高方, 赵南京, 等. 浮游藻类细胞显微场图像与荧光同步测量图像配准方法研究[J]. 中国激光, 2022, 49(24): 2407202.
Jia R Q, Yin G F, Zhao N J, et al. Registration method of microscopic bright field and fluorescence synchronous measurement images of phytoplankton cells[J]. Chinese Journal of Lasers, 2022, 49(24): 2407202.
- 於时才, 吕艳琼. 一种图像快速配准算法的研究[J]. 激光与红外, 2009, 39(4): 447-449.
Yu S C, Lü Y Q. Study of image registration fast algorithm[J]. Laser & Infrared, 2009, 39(4): 447-449.

- [20] 陈凡秀, 何小元. 基于时域小波变换相位提取的三维形貌测量[J]. 光学学报, 2006, 26(12): 1803-1806.
Chen F X, He X Y. Instantaneous three-dimensional profile measurement based on temporal wavelet transform[J]. Acta Optica Sinica, 2006, 26(12): 1803-1806.
- [21] 庞博清, 王帅, 杨平. 基于模式系数求解的相位解缠算法研究[J]. 激光与光电子学进展, 2018, 55(11): 111004.
Pang B Q, Wang S, Yang P. Phase unwrapping algorithm based on mode coefficient solution[J]. Laser & Optoelectronics Progress, 2018, 55(11): 111004.
- [22] 朱星申, 宫雪非. 大口径非球面透镜支撑方法的优化[J]. 激光与光电子学进展, 2017, 54(1): 012203.
Zhu X S, Gong X F. Optimization on supporting method of large-aperture aspheric lens[J]. Laser & Optoelectronics Progress, 2017, 54(1): 012203.
- [23] 周游, 王青, 刘世杰. 一种修正孔径拼接中系统误差的方法[J]. 激光与光电子学进展, 2014, 51(5): 051202.
Zhou Y, Wang Q, Liu S J. A method to modify systematic errors in the stitching[J]. Laser & Optoelectronics Progress, 2014, 51(5): 051202.

Phase Extraction Method for Single Interferogram Based on Light Intensity Iteration

Zhang Xiangyu, Tian Ailing, Liu Zhiqiang, Wang Hongjun, Liu Bingcai, Zhu Xueliang*

School of Opto-Electrical Engineering, Shaanxi Province Key Laboratory of Thin Films Technology and Optical Test, Xi'an Technological University, Xi'an 710021, Shaanxi, China

Abstract

Objective Precision optical components are widely employed in various optical systems, and the surface shape quality of optical components directly affects the performance of optical devices. Therefore, surface shape detection of optical components is of great significance. Interferometry is widely recognized as the most effective method for surface shape detection, among which phase-shifting interferometry has higher detection accuracy. However, during the continuous collection of multiple interferograms with phase differences, it is constrained by the performance of the phase-shifting components and easily affected by such objective factors as mechanical vibration and air disturbance in the environment, which decreases the detection accuracy. Therefore, it is not suitable for on-site production testing. In recent years, researchers have proposed a method that combines carrier interferometry with Fourier analysis technology to achieve phase extraction of a single interferogram. However, generally, there are still shortcomings such as large tilt direction edge errors, stripe stacking phenomenon, and low recovery accuracy. To solve the problem of low accuracy in phase extraction of single interferograms in the above phase-solving methods, we propose a new single interferogram phase extraction method based on light intensity iteration. Meanwhile, simulations and experimental research are conducted, with the stability of the algorithm analyzed.

Methods We adopt a combination of simulation and experiment methods, analyze and explore the principle of the light intensity iteration method, and employ MATLAB to write algorithm programs while conducting simulation verification. The feasibility, stability, and noise resistance of the algorithm are explored via simulations to ensure the algorithm performance. By conducting 100 sets of simulation simulations, the final phase residuals are compared, and the convergence conditions suitable for solving single interference fringes and the solution interval with the best measurement performance are obtained. To ensure the innovation and optimization ability of the algorithm, we conduct a comparison with the Fourier transform method. Finally, multiple experiments are carried out using the ZYGO-Verifire PE phase-shifting interferometer to measure optical components. Multiple sets of experiments are conducted in an experimental environment with temperature of 23 °C and air humidity of 75.3%. Meanwhile, a single interference fringe pattern is collected and the phase is solved using the proposed algorithm. The results are compared, and the effectiveness of the algorithm is evaluated by residual PV and RMS values to achieve phase extraction of the single interference fringe.

Results and Discussions Our algorithm can ensure the algorithm stability while improving detection accuracy. By adopting the Bernsen algorithm to binarize the original interferogram and further obtain a stepped predicted phase (Fig. 3), initial information is provided for subsequent light intensity iterations. The use of binarization to predict phases provides a new approach for iterative methods. The feasibility and anti-noise ability of this method are demonstrated by comparing it with the Fourier transform method (Fig. 4). Compared with the Fourier transform method, the proposed method has higher solving accuracy and faster solving speed. Meanwhile, its anti-noise ability is not significantly different from that of the Fourier method, both of which have sound anti-noise ability. By conducting hundreds of simulation experiments,

convergence conditions that do not affect computational efficiency and avoid excessive iterations are obtained. The study on the effect of the fringe number on the accuracy of the algorithm solution shows that generally the size of the algorithm residual presents a trend of first decreasing and then increasing with the rising number of fringes (Fig. 8). Data comparison shows that the algorithm has the highest solution accuracy when processing a single interference fringe pattern with 4 to 5 fringes.

Conclusions We propose a phase solution method based on the light intensity iteration method. Firstly, the original interferogram is binarized and the initial phase is obtained by phase unwrapping. Then, the background light and modulated light are preliminarily estimated by adopting the least square method using the interference intensity expression. The measured phase is calculated using a variation of the interference intensity expression. The measured phase is compared with the initial phase as a convergence judgment. The initial phase is replaced with a surface shape that does not meet the accuracy requirements. The background light and modulated light are updated, and the phase solution process is repeated. By light intensity iteration, the phase is extracted from a single interferogram. Meanwhile, solution accuracy, noise resistance, and algorithm stability are simulated and analyzed. Experimental measurements are conducted on a 100 mm planar element, and the results show that the obtained phase distribution of the proposed method is consistent with the phase obtained by the four-step phase-shifting algorithm of the ZYGO-Verifire PE phase-shifting interferometer. Compared to those obtained by the interferometer, the residual PV and RMS values obtained by the light intensity iteration method are 2.49 nm and 0.35 nm respectively. This indicates that the proposed method featuring high stability and efficiency can extract phase distribution from single fringes and can meet the testing needs of the production site environment.

Key words measurement; interferometry measurement; single interferogram; iterative method; least square method